Topography and Tomography of Keratoconus

10

Shizuka Koh

10.1 Introduction

In the human eye, aberrations and light scattering are the primary factors in the degradation of optical quality. In eyes with diseases of the ocular surface or anterior segment, the irregularity of the refractive surfaces, such as anterior/posterior corneal surfaces or the precorneal tear film, can cause increased irregular astigmatism, higher-order aberrations (HOAs), or increased light scattering. Corneal haze with decreased corneal transparency is associated with increased ocular scattering. Clinically, corneal haze is typically estimated as corneal backward light scattering, as observed via slit-lamp examination. In contrast, the detection of a subtle distortion of the corneal shape in a clear cornea without abnormal clinical slit-lamp signs is challenging. Corneal topography is mandatory in such cases.

Thus, corneal topography in clinical practice aims (a) to measure corneal power, (b) to diagnose preexisting corneal irregular astigmatism, and (c) to assess the effect of increased irregular astigmatism or HOAs on the optical quality of the entire eye.

S. Koh (✉)
Department of Innovative Visual Science, Osaka University Graduate School of Medicine, Osaka, Japan
e-mail: skoh@ophthal.med.osaka-u.ac.jp

10.2 Topography Vs. Tomography

Topography derives from the Greek words *topos* ("place") and *-graphia* ("writing"), which refer to writing about a place. Tomography is derived from the Greek words *tomos* ("section" or "slice") and *-graphia* ("writing"), which refer to writing about a section (slice). In ophthalmic medicine, corneal topography only provides two-dimensional information about the frontal surface of the cornea, whereas corneal tomography visualizes a three-dimensional section of the cornea [1, 2].

10.2.1 Historical Background

Computerized video keratography for the diagnosis of keratoconus was first introduced in the 1980s. Early systems relied on the analysis of Placido disk images to compute the anterior corneal curvature [3]. It has represented a true revolution in the diagnosis and management of corneal diseases, including keratoconus. The advent of refractive surgery and the coincident risk of iatrogenic ectasia or unmasking of keratoconus spurred the development of newer diagnostic devices aimed at the early detection of subclinical keratoconus. The Orbscan (Bausch and Lomb, Rochester, NY, USA) utilized slit-scanning technology to provide wide-field pachymetry, anterior and posterior elevation, and keratometry maps. In a later iteration, Orbscan II

S. Das (ed.), *Keratoconus*, https://doi.org/10.1007/978-981-19-4262-4_10

combines slit scanning with Placido-based topography analysis. The Scheimpflug principle has been exploited in corneal tomographers to provide a three-dimensional mapping of the cornea, including direct measurement of anterior and posterior corneal surfaces, pachymetry, and anterior chamber angle characterization. Swept-source/Fourier domain optical coherence tomography devices have been introduced with higher speed and sensitivity, allowing anterior and posterior corneal topography as well as cross-sectional corneal images.

As previously mentioned, corneal topography is used to characterize the shape of the anterior surface of the cornea. Currently, even when the data of the corneal shape are obtained using corneal "tomography"-based devices, terms such as "corneal topography" can be found in the literature. In this way, "corneal topography" is used broadly to mean the characterization of the shape of the cornea, close to "corneal shape imaging" (Fig. 10.1). Therefore, it is always important to make sure whether "topography" or "tomography" is used when observing the description of "corneal topography."

This chapter focuses on the basics of the most commonly used three "corneal topography" techniques: Placido-based corneal topographer, Scheimpflug-based tomography, and anterior segment optical coherence tomography (OCT).

10.3 Placido-Based Corneal Topographer

10.3.1 Principle

A Placido-based corneal topographer, previously referred to as a videokeratoscope, analyzes the contours of the anterior corneal surface [4]. It is based on the Placido disk principle. A Placido disk is a device made of concentric rings drawn on a device of different colors. The name Placido is derived from the name of a Portuguese ophthal-

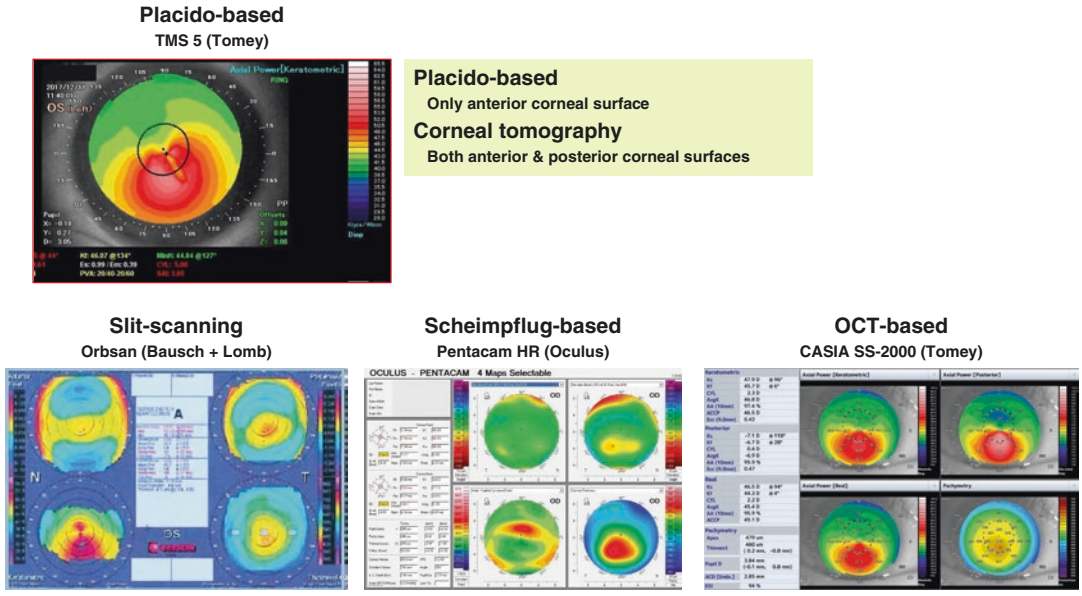

Fig. 10.1 Principles used for the characterization of the shape of the cornea

mologist, Dr. Antonio Placido, who developed this in the late 1800s [5]. It was developed to overcome the shortcomings of the keratometers, which typically measure the average curve of the central 3 mm of the cornea in two meridians. This includes at least three limitations with the keratometer: (a) measures curves that are not equivalent to shape, (b) evaluates the average central curves instead of a true measurement, and (c) implies a very small area compared to the ocular surface. Computerized Placido-based topographers assess the reflection of a circular mire of concentric lighted rings projected onto the air-tear film interface. The radii of the anterior corneal curvature and the axis of astigmatism were determined by analyzing the size and toricity of the mire, similar to the keratometers. Placido-based topographers provide a qualitative and quantitative description of the morphology of the cornea in a color-coded topographical map based on the power across an extensive area of the cornea based on the mires [4, 6].

10.3.2 Features

- Since it uses the same principle as a keratometer, simulated K readings can be indicated as the compatible index of K readings; however, these two indices are not always interchangeable.
- Placido-based corneal topographers quickly obtain the image created at the precorneal tear film in a single shot, which contributes to the good reproducibility of the data. In contrast, Placido-based topographic maps are subject to fluctuations in tear film stability. Therefore, caution is needed when measuring dry eyes or eyes with decreased tear film stability. Previous researchers have reversely used this phenomenon as sequential measurements of corneal topographic data [7, 8].
- It is challenging for the videokeratoscope to digitize heavily distorted mire images in eyes with severe irregular astigmatism.
- Since it can provide information on only the anterior corneal surface, Placido-based corneal topographers cannot identify highly mild forms of keratoconus (generally defined as forme fruste keratoconus), which would require identification, assessing at least the corneal thickness and posterior curvature measurements with corneal tomography described later.

10.3.3 Application Tools for Keratoconus Management

- **Keratoconus Screening Program.**
  A variety of indices were developed for discriminating keratoconus from normal eyes, such as superior-inferior asymmetry value (I-S value) of less than 1.4 at 6 mm (3-mm radii), keratoconus percentage index, Klyce/Maeda keratoconus index, and Smolek/Klyce keratoconus severity index [9–12].

In Fig. 10.2, the keratoconus screening display obtained in a patient with keratoconus is also demonstrated. While her right eye exhibited clinical keratoconus, there was no abnormal finding on the slit-lamp examination of her left eye. However, the keratoconus screening program using Placido-based corneal topography detected keratoconus in her left eye. Although specialty clinics or the screening of refractive surgical patients require further corneal assessment using corneal tomography, the early detection of keratoconus or corneal ectasia is possible using Placido-based corneal topographers in general clinics or primary care.

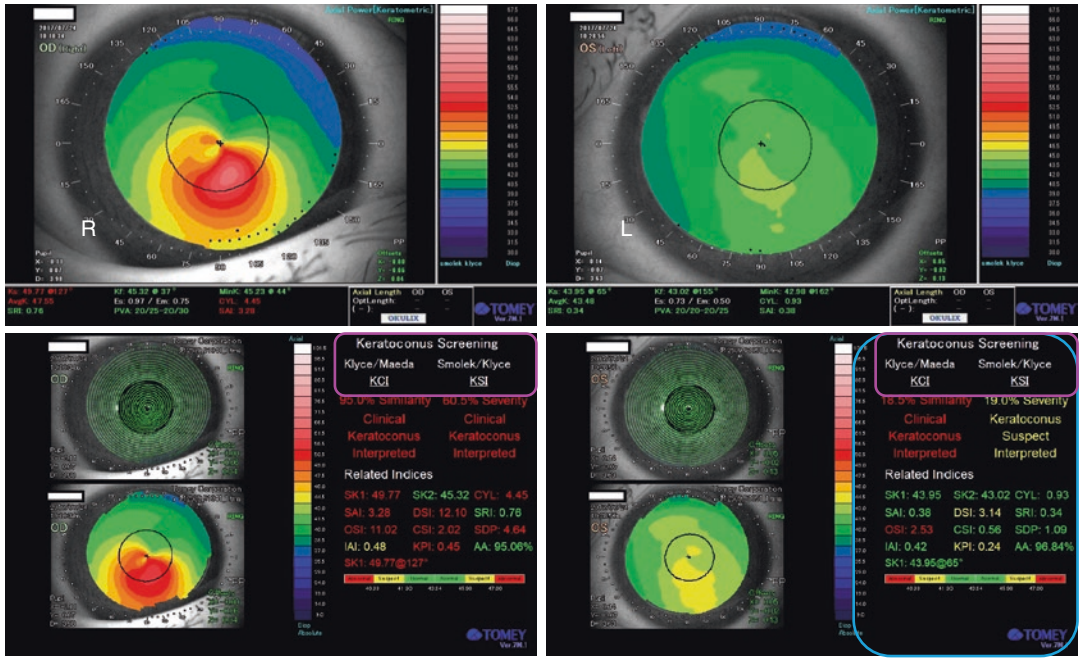

Fig. 10.2 Color-coded topographical map obtained with Placido-based corneal topographer (TMS-5, Tomey). Ring Topo Mode, a Placido-based topography method is used. Upper row panels, original map. Lower row panels, keratoconus screening display

10.4 Scheimpflug-Based Tomography

10.4.1 Principle

Scheimpflug principle [13] eliminates the problem noted with centrally located slit-scanning technology cameras, that there was poor/unreliable capture of the peripheral corneal data, caused by the nonplanar shape of the cornea. The Scheimpflug principle states that when a planar subject is not parallel to the image plane, an oblique tangent can be drawn from the image, object, and lens planes and the point of intersection is called Scheimpflug intersection [2]. The commonly used Scheimpflug-based devices are described in Table 10.1.

The Pentacam HR (OCULUS) is described as an example. A representative color-coded map of keratoconus obtained using Pentacam HR is shown in Fig. 10.3.

10.4.2 Features

- Assessment of clinically relevant parameters such as corneal wavefront aberrations, backward scattering, anterior segment analysis, biometry, and calculation of intraocular lens power is possible.
- Refractive components of the posterior corneal surface and corneal thickness profile can be obtained in addition to the anterior corneal topography.
- The calculation of the total corneal power is possible. For eyes with abnormal corneal shape, appropriate intraocular lens (IOL) power calculation formulae can be applied.
- Corneal scars or haze may scatter visible light (475 nm for Pentacam) in the Scheimpflug-based corneal topographer. Thus, the scattered scanning beam may make it challenging to digitize the corneal surfaces precisely.

Table 10.1 The commercially available, commonly used "corneal tomography" instruments

Technology	Type	Product (manufacturer)
Scheimpflug-based devices	Rotating Scheimpflug	Pentacam Series (OCULUS, Wetzlar, Germany)
		WaveLight® OCULYZER II (Alcon, Texas, USA)
	Hybrid system	Galilei (Ziemer, Port, Switzerland)
		TMS-5 (Tomey, Aichi, Japan)
		Sirius (Costruzione Strumenti Oftalmici, Florence, Italy)
Anterior segment OCT	Time-domain OCT	Visante (Carl Zeiss Meditec, Dublin, California, USA)
	Spectral-domain OCT	RTVue (Optovue Inc., Fremont, California, USA)
	Swept-source OCT	CASIA SS-1000, 2000 (Tomey, Aichi, Japan)
		ANTERION (Heidelberg Engineering, Heidelberg, Germany)

10.4.3 Application Tools for Keratoconus Management

- **Enhanced Ectasia Detection Program**
  The Belin/Ambrósio enhanced ectasia display [14] can be employed for the detection of clinical or subclinical keratoconus (Fig. 10.4). It combines both elevation and pachymetric parameters in a regression analysis. Anterior and posterior elevation data relative to the standard best-fit sphere calculated at a fixed optical zone of 8.0 mm are shown on the left side (orange-lined box). The different elevation maps at the bottom part (navy-lined box) show the relative change in elevation from the standard (baseline). Based on the amount of elevation change, colors in the anterior (front) or posterior (back) corneal surfaces indicate signs such as green (normal), yellow (suspicious), and red (abnormal). In the bottom right of the display (pink-lined box), a series of indices are characterized by a "d" value, which reflect the standard deviation from the mean of a reference population for the following five parameters: Df (front elevation), Db (back elevation), Dp (pachymetric progression), Dt (corneal thickness at thinnest point), and Da (thinnest point displacement). In the BAD D, the final "D" reading represents overall map-reading taken each of these five D parameters into account. If each parameter value exceeds 1.6, it is indicated in yellow (suspicious) and red (abnormal) when the value exceeds 2.6. All D parameters are shown in red in the case of keratoconus (Fig. 10.4).
- **ABCD Keratoconus Grading System**
  This newest classification [15] utilizes four parameters (A to D): anterior (A) and posterior (B) radius of curvature in the 3.0-mm zone centered on the thinnest location of the cornea, thinnest corneal pachymetry (C), and distance best-corrected visual acuity (D). It would be useful to monitor the changes (progression) in keratoconus and assess the efficacy of corneal cross-linking.
- **Tomographic Biomechanical Assessment.**
  Combining Scheimpflug-based corneal tomography with biomechanical data obtained with dynamic Scheimpflug biomechanical analysis (Corvis ST, OCULUS), Tomographic Biomechanical Index (TBI) was calculated using an artificial intelligence approach to optimize ectasia detection [16]. Several studies have demonstrated a higher capability of detecting subclinical (fruste) ectasia among eyes with normal topography in highly asymmetric patients when compared to tomographic analysis alone. The ARV (Ambrósio, Roberts & Vinciguerra) Biomechanical and Tomographic Display showing BAD D (derived from only Pentacam), the Corvis Biomechanical Index (CBI) (derived from only Corvis ST), and TBI. The case shown in Fig. 10.5 is a fellow eye with highly asymmetric ectasia with clinical ectasia in the one eye and a fellow eye with normal topography with-

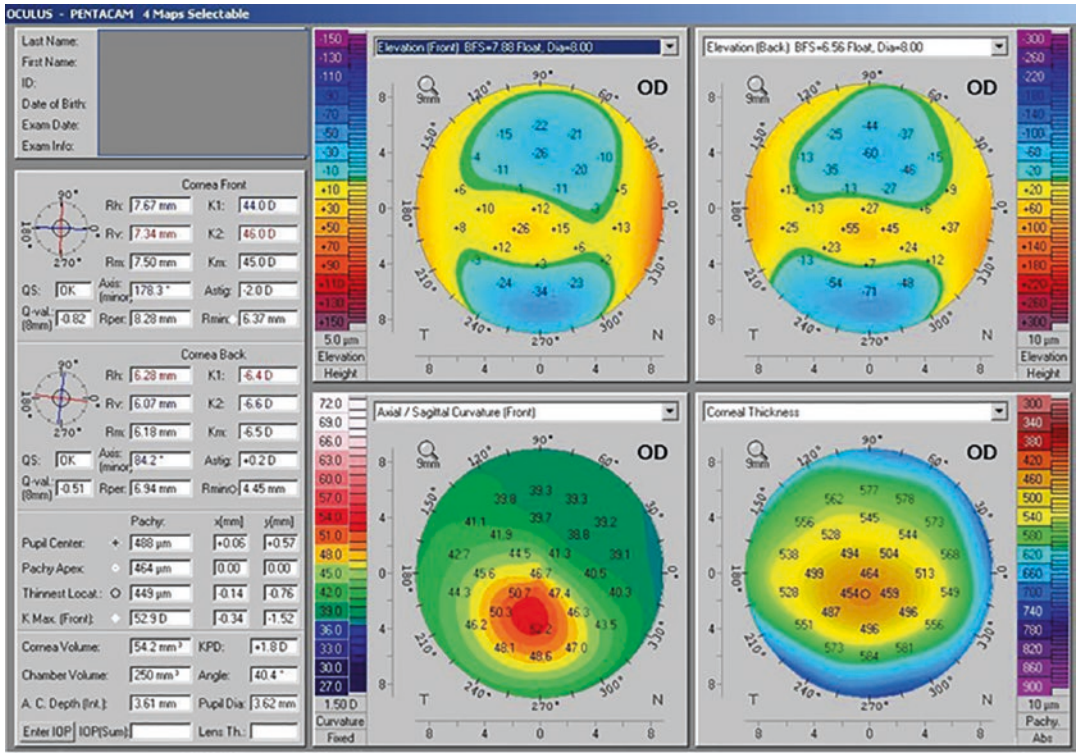

Fig. 10.3 Color-coded map of keratoconus obtained using a rotating Scheimpflug camera (Pentacam HR, OCULUS). Four maps are shown: anterior and posterior elevation maps, axial power maps, and pachymetry maps

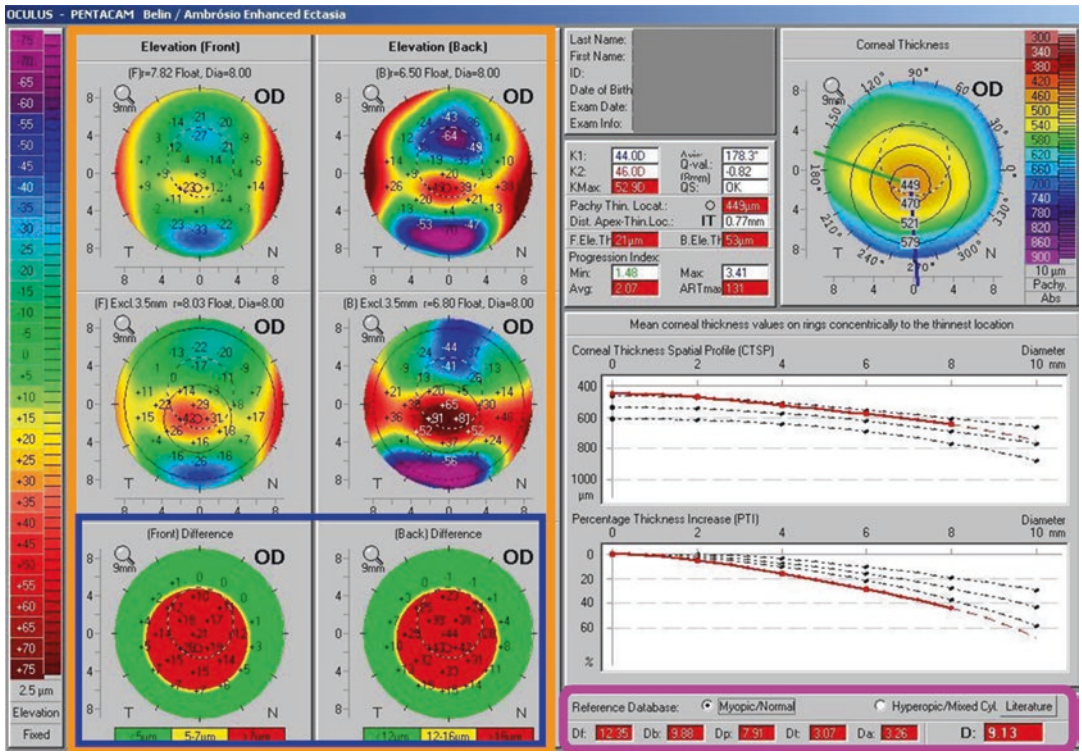

Fig. 10.4 The Belin/Ambrósio Enhanced Ectasia Display (Pentacam HR, OCULUS) for the same data (Fig. 10.3)

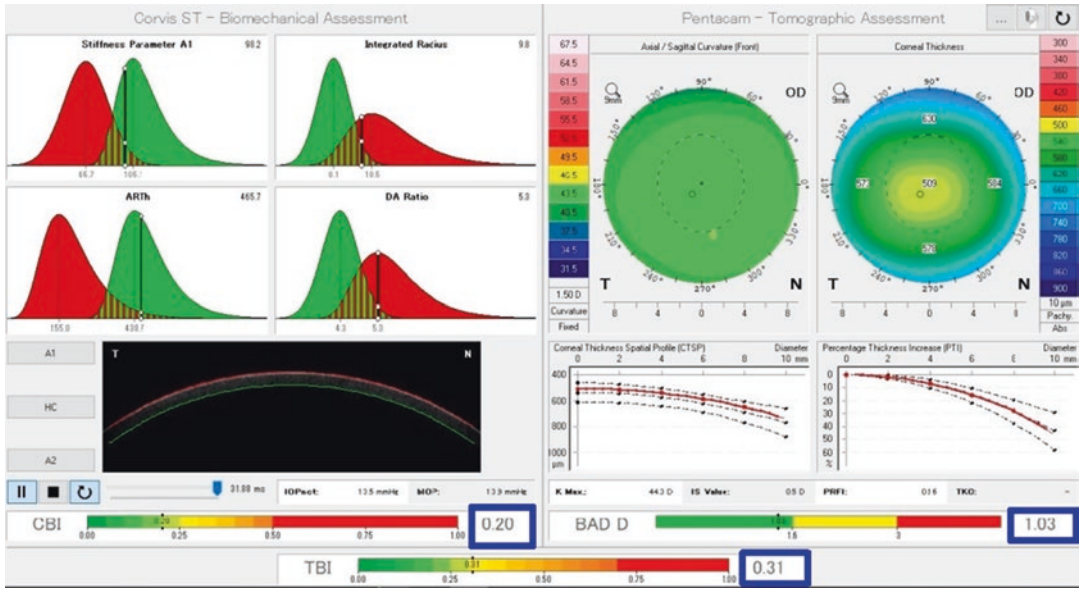

Fig. 10.5 The ARV (Ambrósio, Roberts & Vinciguerra) Biomechanical and Tomographic Display from dynamic Scheimpflug biomechanical analysis (Corvis ST, OCULUS)

out clinical signs [17]. Based on the reported cutoff values (BAD D, 1,6; CBI, 0.5; TBI, 0.29) [16, 18, 19], both BAD D (1.03) and CBI (0.20) values are normal; however, the TBI value (0.31) is suspicious. Thus, subclinical ectasia is detected only in patients with TBI.

10.5 Anterior Segment OCT

10.5.1 Principle

The first report of OCT imaging of the cornea and anterior segment was published in 1994 [20]. OCT can be categorized into two types: time-domain OCT and Fourier-domain OCT. Similar to OCT for retinal imaging, time-domain OCT at 1310 nm was initially introduced for cross-sectional images of the anterior segment of the eye. With the commercial introduction of the 840-nm spectral-domain OCT, imaging of the anterior segment at much higher speeds (>25,000 A-scans/s), and better axial resolution (5 μm) became feasible. However, spectral-domain OCTs use shorter wavelength light sources, optimized for posterior segment imaging, resulting in a more limited image depth range and area [21]. Later, 1310-nm swept-source OCT based on the Fourier-domain OCT type has become commercially available, making it feasible to reconstruct the three-dimensional images of the anterior segment of the eye more precisely and faster [22]. The current generation of spectral-domain OCT devices widely used by clinicians to image the posterior segment can also acquire anterior segment images using anterior segment lenses or attachments. The commonly used Scheimpflug devices are listed in Table 10.1.

CASIA SS-2000 (Tomey) is described as an example. A representative color-coded map of keratoconus obtained using CASIA SS-2000 is shown in Fig. 10.6.

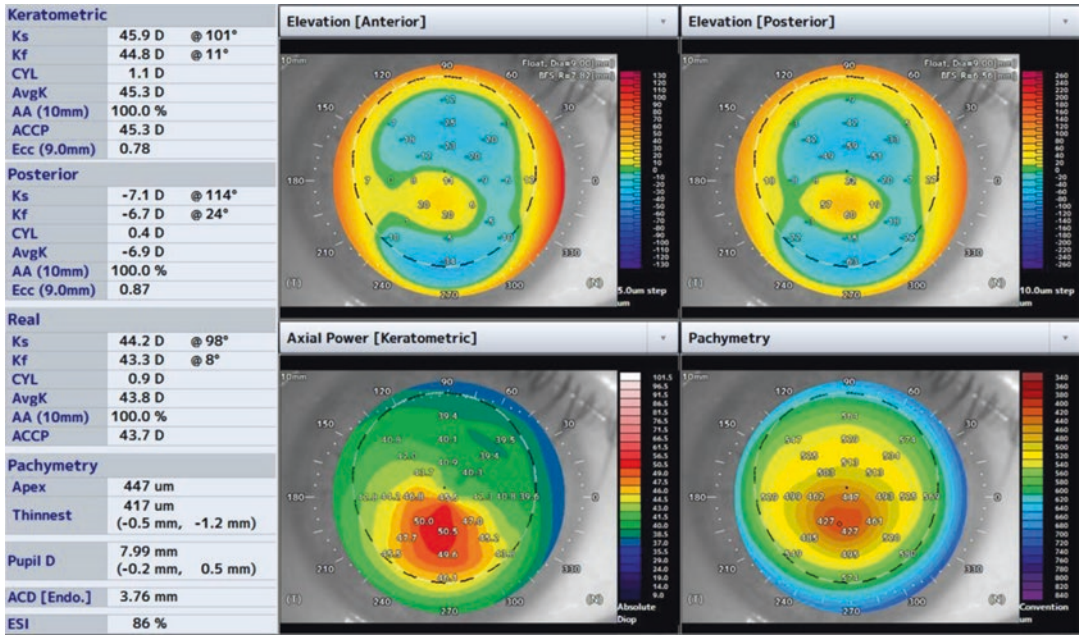

Fig. 10.6 Color-coded map of keratoconus obtained using optical coherence tomography (CASIA SS-2000, Tomey). The same case as in Figs. 10.3 and 10.4. Four maps are shown: anterior and posterior elevation maps, axial power maps, and pachymetry maps

10.5.2 Feature

- The assessment of clinically relevant parameters such as corneal curvature, corneal wavefront aberrations, anterior segment analysis, biometry, and calculation of intraocular lens power is possible.
- With the use of OCT, topographic analysis can be performed even in the area of a severe scar/haze or even when edema exists in the corneal stroma (Fig. 10.7) [23]. This may be a potential advantage of the OCT corneal topographer over other devices for evaluating various types of corneal diseases or eyes, including pre-and post-corneal surgeries.

10.5.3 Application Tools for Keratoconus Management

The application of OCT in clinical practice has been steadily increasing. Herein, unique application tools for keratoconus management are introduced.

- **Fourier Series Harmonic Analysis**
  It can separate and quantify the refractive components of the cornea [24]. Dioptric data from the original color-coded map is expanded into spherical, regular astigmatism, asymmetry, and higher-order irregularity components using Fourier analysis (Fig. 10.8). Among them, asymmetry and higher-order irregularity are components of irregular astigmatism. Fourier indices from the anterior corneal surface in the upper panel, posterior corneal surface in the middle panel, and total cornea in the lower panel are shown in this display. The magnitudes of the Fourier indices of the central 3 and 6 mm of the cornea were indicated and colored as green meaning within the normal range, yellow meaning borderline, and red meaning abnormal. The case presented in Fig. 10.8 is a representative Fourier map captured using OCT in a keratoconic eye.

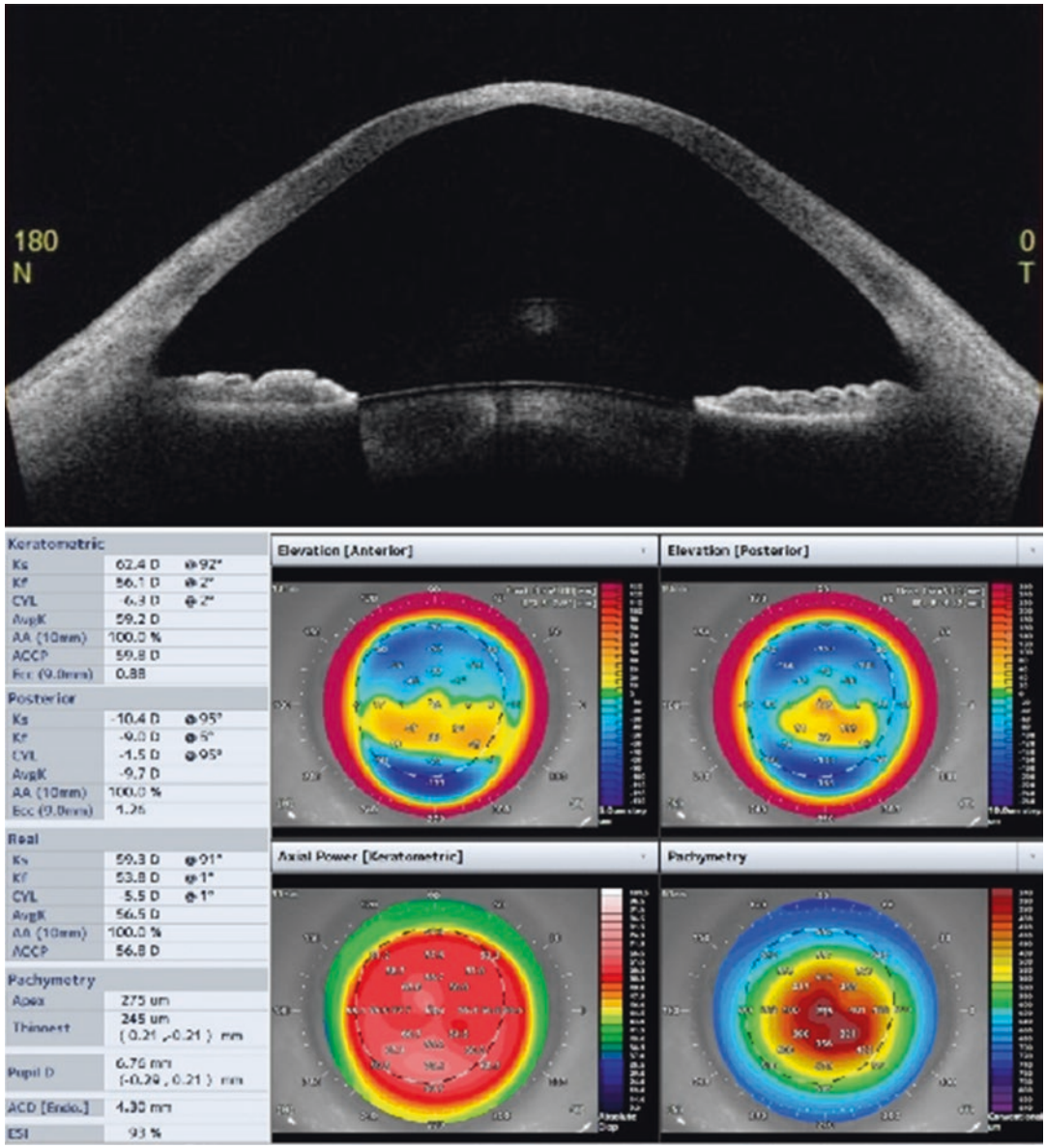

Fig. 10.7 Optical coherence tomography (OCT) image obtained using OCT (CASIA SS-2000, Tomey) for keratoconus with corneal haze after acute hydrops

Moreover, corneal topographical analysis during contact lens wear is possible using OCT (Fig. 10.9). Posterior corneal surface flattening associated with alteration of corneal biomechanics in the corneal stroma during corneal rigid gas-permeable contact lens wear has been reported recently [24].

- **Trend Analysis**
  This application can perform trend analysis of the time course changes patients' corneas based on topographic quantitative parameters [25]. It is useful as a trend analysis tool for keratoconus progression evaluation, corneal cross-linking preoperative indication judgment, and preoperative and postoperative assessment.

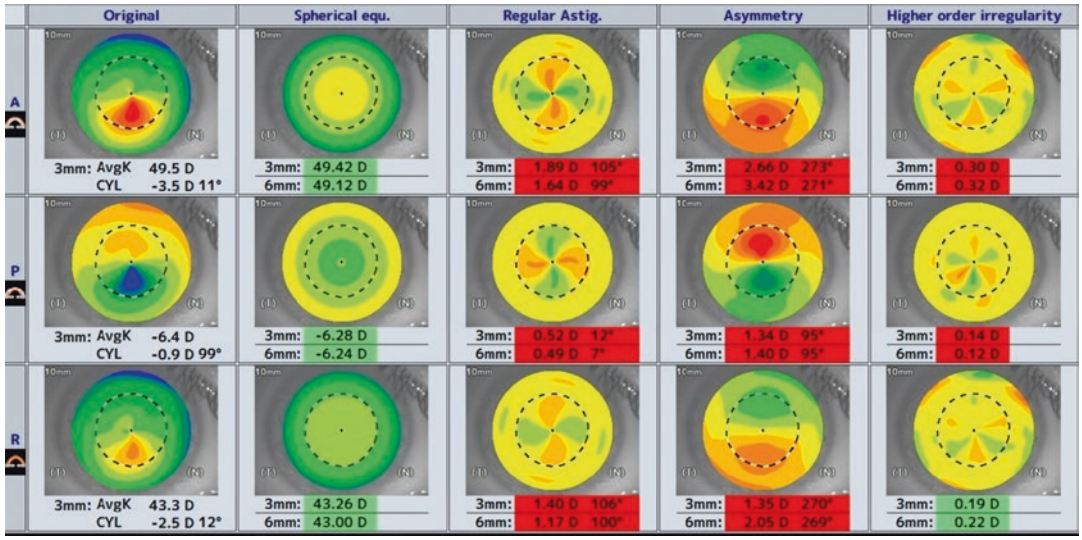

Fig. 10.8 Fourier maps from optical coherence tomography (OCT) (CASIA SS-2000, Tomey) in a keratoconic eye

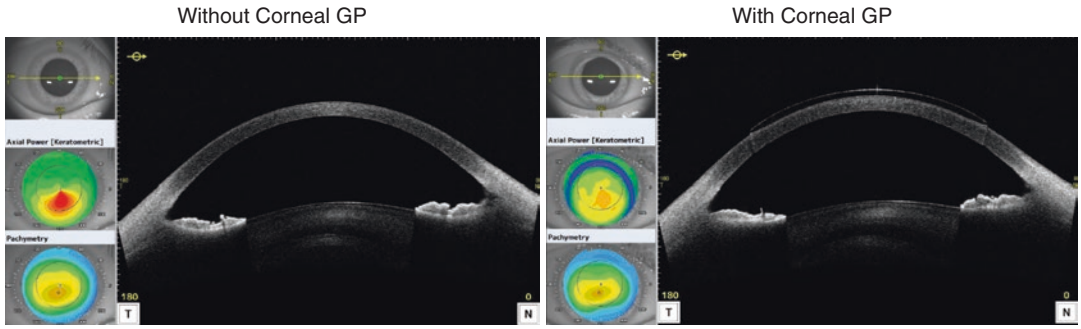

Fig. 10.9 Optical coherence tomography (OCT) images obtained using OCT (CASIA SS-2000, Tomey) for keratoconus with and without corneal rigid gas-permeable contact lens. The same case as in Fig. 10.8

- **Corneal Rigid Gas-Permeable Contact Lenses Fitting Software**
  "Itoi Method of HCL Fitting Software" of CASIA SS-2000 displays can suggest the appropriate base curve values for keratoconus with respect to the lens diameter, based on the corneal tomographic data.

10.6 Combined Systems with a Wavefront Aberrometer

Combined systems of corneal topographers or tomographers with wavefront aberrations that can measure wavefront aberrations of the whole eye are available. KR-1 W (Topcon, Tokyo, Japan) and OPD-Scan (Nikon, Aichi, Japan) integrated a Placido-based topography system and a wavefront aberrometer. The Pentacam AXL Wave (OCULUS) is a combination system that contains a rotating Scheimpflug-based corneal tomography system and a wavefront aberrometer.

10.7 Tips for the Measurements

- The patient fixation during the measurement should be considered.
- The ocular surface and tear film should be ensured to be stable. The patient should

be asked to blink naturally before the measurements.
- The patient should be instructed to open his or her eyes wide, and the upper eyelids or eyelashes should be ensured to be unaffected.
- The measurements should be repeated, and the repeatability should be verified.

10.8 Tips at Reading the Maps

- The quality of the measurements should be checked. In advanced keratoconus or keratoconus with corneal opacity, it is challenging to precisely digitize the corneal surfaces using a Placido-based corneal topographer or Scheimpflug-based tomography, leading to the low reliability of the measurements.
- The color-coded scale [26] for the maps should be checked. Generally, a color palette can be chosen such that lower corneal powers are represented by cooler colors (blue shades), while higher corneal powers are represented by warmer colors (red shades). Green shades represent the corneal powers associated with normal corneas. When comparing the different maps, the same scale must be used; otherwise, even when the change is the same, it can be overestimated or underestimated.
- It is important to observe the topography images of normal eyes without corneal diseases, as there are variations even in normal eyes.

10.9 Final Practical Comment from Specialists

Ophthalmology is a rapidly advancing field with new technologies for diagnosis and treatment. As more advanced techniques develop, the utility of advanced corneal imaging techniques continues to grow. Multimodal imaging should be always applied in detection and diagnosis of subclinical or clinical keratoconus [27]. However, understanding the fundamental tools is always important, and we have to respect previous researchers.

References

1. Ambrósio R Jr, Belin MW. Imaging of the cornea: topography vs tomography. J Refract Surg. 2010;26(11):847–9.
2. Fan R, Chan TC, Prakash G, Jhanji V. Applications of corneal topography and tomography: a review. Clin Exp Ophthalmol. 2018;46(2):133–46.
3. American Academy of Ophthalmology. Corneal topography. Ophthalmology. 1999;106(8):1628–38.
4. Klyce SD. Computer-assisted corneal topography. High-resolution graphic presentation and analysis of keratoscopy. Invest Ophthalmol Vis Sci. 1984;25(12):1426–35.
5. Placido A. Neue Instrumente. Centralbl Prakt Augenheilkd. 1882;6:30–1.
6. Wilson SE, Klyce SD. Quantitative descriptors of corneal topography. A clinical study. Arch Ophthalmol. 1991;109(3):349–53.
7. Németh J, Erdélyi B, Csákány B, Gáspár P, Soumelidis A, Kahlesz F, Lang Z. High-speed videotopographic measurement of tear film build-up time. Invest Ophthalmol Vis Sci. 2002;43(6):1783–90.
8. Goto T, Zheng X, Klyce SD, Kataoka H, Uno T, Karon M, Tatematsu Y, Bessyo T, Tsubota K, Ohashi Y. A new method for tear film stability analysis using videokeratography. Am J Ophthalmol. 2003;135(5):607–12.
9. Maeda N, Klyce SD, Smolek MK, Thompson HW. Automated keratoconus screening with corneal topography analysis. Invest Ophthalmol Vis Sci. 1994;35(6):2749–57.
10. Maeda N, Klyce SD, Smolek MK. Comparison of methods for detecting keratoconus using videokeratography. Arch Ophthalmol. 1995;113(7):870–4.
11. Smolek MK, Klyce SD. Current keratoconus detection methods compared with a neural network approach. Invest Ophthalmol Vis Sci. 1997;38(11):2290–9.
12. Rabinowitz YS, Rasheed K. KISA% index: a quantitative videokeratography algorithm embodying minimal topographic criteria for diagnosing keratoconus. J Cataract Refract Surg. 1999;25(10):1327–35.
13. Wegener A, Laser H. Imaging of the spatial density distribution on the capsule of the lens with Scheimpflug photography. Ophthalmic Res. 1996;28(Suppl 2):86–91.
14. Lopes BT, Ramos IC, Dawson DG, Belin MW, Ambrósio R Jr. Detection of ectatic corneal diseases based on Pentacam. Z Med Phys. 2016;26(2):136–42.
15. Belin MW, Duncan J, Ambrósio R Jr, Gomes JAP. A new tomographic method of staging/classifying keratoconus: the ABCD grading system. Int J Kerat Ect Cor Dis. 2015;4(3):85–93.
16. Ambrósio R Jr, Lopes BT, Faria-Correia F, Salomão MQ, Bühren J, Roberts CJ, Elsheikh A, Vinciguerra R, Vinciguerra P. Integration of Scheimpflug-based corneal tomography and biomechanical assessments for enhancing ectasia detection. J Refract Surg. 2017;33(7):434–43.

17. Koh S, Ambrósio R Jr, Inoue R, Maeda N, Miki A, Nishida K. Detection of subclinical corneal ectasia using corneal tomographic and biomechanical assessments in a Japanese population. J Refract Surg. 2019;35(6):383–90.
18. Villavicencio OF, Gilani F, Henriquez MA, Izquierdo L, Ambrósio RR. Independent population validation of the Belin/Ambrósio enhanced ectasia display: implications for keratoconus studies and screening. Int J Kerat Ect Cor Dis. 2014;3(1):1–8.
19. Vinciguerra R, Ambrósio R Jr, Elsheikh A, Roberts CJ, Lopes B, Morenghi E, Azzolini C, Vinciguerra P. Detection of keratoconus with a new biomechanical index. J Refract Surg. 2016;32(12):803–10.
20. Izatt JA, Hee MR, Swanson EA, Lin CP, Huang D, Schuman JS, Puliafito CA, Fujimoto JG. Micrometer-scale resolution imaging of the anterior eye in vivo with optical coherence tomography. Arch Ophthalmol. 1994;112(12):1584–9.
21. Maeda N. Optical coherence tomography for corneal diseases. Eye Contact Lens. 2010;36(5):254–9.
22. Yasuno Y, Madjarova VD, Makita S, Akiba M, Morosawa A, Chong C, Sakai T, Chan KP, Itoh M, Yatagai T. Three-dimensional and high-speed swept-source optical coherence tomography for in vivo investigation of human anterior eye segments. Opt Express. 2005;13(26):10652–64.
23. Nakagawa T, Maeda N, Higashiura R, Hori Y, Inoue T, Nishida K. Corneal topographic analysis in patients with keratoconus using 3-dimensional anterior segment optical coherence tomography. J Cataract Refract Surg. 2011;37(10):1871–8.
24. Koh S, Inoue R, Maeda N, Oie Y, Jhanji V, Miki A, Nishida K. Corneal tomographic changes during corneal rigid gas-permeable contact lens wear in keratoconic eyes. Br J Ophthalmol. 2022;106(2):197–202.
25. Fujimoto H, Maeda N, Shintani A, Nakagawa T, Fuchihata M, Higashiura R, Nishida K. Quantitative evaluation of the natural progression of keratoconus using three-dimensional optical coherence tomography. Invest Ophthalmol Vis Sci. 2016;57(9):OCT169-175.
26. Wilson SE, Klyce SD, Husseini ZM. Standardized color-coded maps for corneal topography. Ophthalmology. 1993;100(11):1723–7.
27. Ambrósio R Jr. Multimodal imaging for refractive surgery: *quo vadis?* Indian J Ophthalmol. 2020;68(12):2647–9.